CHINESE OPTICS LETTERS

Vol. 22, No. 3 | March 2024

Stimulated emission–depletion-based point-scanning structured illumination microscopy

Lei Wang (汪 磊)[1,2,†], Meiting Wang (王美婷)[1,†], Luwei Wang (王璐玮)[3], Xiaomin Zheng (郑晓敏)[3], Jiajie Chen (陈嘉杰)[3*], Wenshuai Wu (吴文帅)[3], Wei Yan (严 伟)[3], Bin Yu (于 斌)[3], Junle Qu (屈军乐)[3], Bruce Zhi Gao (高 志)[4], and Yonghong Shao (邵永红)[3**]

[1] Guangdong Key Laboratory for Biomedical Measurements and Ultrasound Imaging, National-Regional Key Technology Engineering Laboratory for Medical Ultrasound, School of Biomedical Engineering, Shenzhen University Medical School, Shenzhen 518060, China

[2] Key Laboratory of Opto-electronic Information Science and Technology of Jiangxi Province, Nanchang Hangkong University, Nanchang 330063, China

[3] College of Physics and Optoelectronics Engineering, Key Laboratory of Optoelectronic Devices and Systems of Ministry of Education and Guangdong Province, Shenzhen University, Shenzhen 518060, China

[4] Department of Bioengineering and COMSET, Clemson University, Clemson SC 29634, US

[†] These authors contributed equally to this work.

*Corresponding author: cjj@szu.edu.cn

**Corresponding author: shaoyh@szu.edu.cn

Received October 6, 2023 | Accepted October 26, 2023 | Posted Online March 13, 2024

Wide-field linear structured illumination microscopy (LSIM) extends resolution beyond the diffraction limit by moving unresolvable high-frequency information into the passband of the microscopy in the form of moiré fringes. However, due to the diffraction limit, the spatial frequency of the structured illumination pattern cannot be larger than the microscopy cutoff frequency, which results in a twofold resolution improvement over wide-field microscopes. This Letter presents a novel approach in point-scanning LSIM, aimed at achieving higher-resolution improvement by combining stimulated emission depletion (STED) with point-scanning structured illumination microscopy (psSIM) (STED-psSIM). The according structured illumination pattern whose frequency exceeds the microscopy cutoff frequency is produced by scanning the focus of the sinusoidally modulated excitation beam of STED microscopy. The experimental results showed a 1.58-fold resolution improvement over conventional STED microscopy with the same depletion laser power.

Keywords: stimulated emission depletion; structured illumination microscopy; superresolution microscopy.
DOI: 10.3788/COL202422.031701

1. Introduction

Fluorescence microscopy's noncontact detection and real-time imaging characteristics are widely used in biological science to observe the structure of cells and tissues. However, the resolution of fluorescence microscopy is restricted by the Abbe limit and generally exceeds 200 nm, which greatly constrains its application. Fortunately, a series of superresolution microscopy imaging techniques have been developed, allowing observation of cellular and subcellular fine structures that are inaccessible to conventional optical microscopy.

Stochastic optical reconstruction microscopy (STORM) proposed by Rust *et al.*[1] and the fluorescence photoactivated localization microscopy (PALM) proposed by Hess *et al.*[2,3] follow a similar principle. Further, both can control the sparse luminescence of fluorescent molecules. Thus within a diffraction limit[4], the phenomenon that two molecules emit light at the same time hardly occurs[5], thereby making these molecules distinguishable in the time domain. The superresolution image can be reconstructed by obtaining the position of each fluorescent molecule through multiple imaging and positioning. The resolution of this type of technology depends on positioning accuracy and can exceed 10 nm[6]. Unfortunately, both STORM and PALM require tens of thousands of images, greatly increasing their imaging time and limiting their application in live-cell imaging.

In 2000, Gustafsson proposed wide-field structured illumination microscopy (SIM)[7], in which the typically unobservable high spatial frequency information of the sample is moved within the microscope's bandpass by illuminating the sample with a sinusoidal stripe pattern[8]. After taking raw images under different phase shifts and orientations of the illumination pattern projected into the sample, and then performing the appropriate deconvolution, we can reconstruct a superresolution image based on the SIM algorithm[9,10]. In linear SIM, three

illumination patterns with a phase difference of $2\pi/3$ are required to increase imaging resolution in a single direction. To obtain an isotropic superresolution image, at least three orientations are needed. Nine raw images are normally required for an isotropic superresolution image. Therefore, linear SIM has a faster imaging speed than either STORM or PALM. Moreover, linear SIM offers a low laser power density that is 2 to 3 orders of magnitude lower than that of STORM or PALM. However, such a wide-field scheme typically is incompatible with point-scanning-based microscopy. Recently, SIM was introduced into scanning microscopy by developing scanning patterned illumination microscopy and scanning patterned detection microscopy[11,12], which extend the concept of spatially inhomogeneous imaging systems to laser scanning microscopes with spatial or temporal modulation. Nevertheless, the resolution improvement factor of linear SIM is twice as high as that of wide-field microscopy because the spatial frequency of the illumination pattern cannot exceed the observable passband of microscopes. Recently, our group introduced the nonlinear effects of the multiphoton fluorescence or second-harmonic generation processes into point-scanning SIM to further improve the resolution up to threefold as much as wide-field microscopy[13–15].

In the stimulated emission depletion (STED) technique proposed by Hell *et al.* in 1994 and realized in 2000[16,17], a high-intensity doughnut-shaped spot depletion beam with a very low (ideally zero) intensity at the center was used to enclose the excitation beam, thereby selectively suppressing fluorescence emission in the beam periphery and subsequently reducing the effective point spread function (PSF) size of the system. The typical STED resolution range is 30 to 70 nm as recorded with the commercial STED systems such as Leica TCS SP8 STED, Abberior's STED systems, and several custom-built STED systems[18].

To improve the resolution of STED under the low-power depletion laser, several techniques have been developed. For example, the combination of STED and SIM can be theoretically analyzed, such as surface plasmon resonance-based STED-SIM[19] and both structured excitation light and structured STED light-based STED-SIM[20]. Localization with stimulated emission depletion (LocSTED) microscopy achieves 15 nm resolution[21]. ExSTED, a combination of expansion microscopy (ExM), which expands the sample physically, and STED achieves an increment in resolution of up to 30-fold compared to conventional microscopy ($<$ 10 nm lateral and ~50 nm isotropic)[22]. ExSTED imaging of microtubules in BS-C-1 cell line achieves 18 nm resolution[23]. Continuing this trend, extremely bright expansion nanoscopy with 10 nm resolution was designed by using biotin avidin signal amplification[24].

In this Letter, a novel superresolution imaging technology that combines STED and point-scanning SIM (STED-psSIM) is reported. The motivation for combining STED and SIM techniques lies in the potential to achieve superresolution imaging with high resolution and reduced photobleaching. STED microscopes excel at achieving ultrahigh spatial resolution but require high optical power, are sensitive to photobleaching, and are stringent in dye selection. At equivalent optical power levels, STED-psSIM can attain even higher resolution while effectively mitigating photobleaching. This enables extended imaging durations and minimizes damage to fluorophores, a critical advantage for dynamic studies or prolonged imaging of delicate specimens, such as living cells. For SIM, in contrast to some other superresolution techniques, SIM possesses the distinct advantage of not necessitating the use of specialized markers or fluorescent molecules. The simplicity of the device and its easy integration with other optical systems are notable attributes. However, SIM has a constraint in its lateral resolution, which may not achieve the same level as certain other superresolution techniques. SIM reaches a lateral resolution approximately twice that of the diffraction limit. STED-psSIM can further enhance the resolution achievable with SIM. Based on the optical setup of conventional STED microscopy, an electro-optic modulator was inserted into the excitation light path to sinusoidally modulate excitation light intensity. In this way, scanning structured illumination patterns were produced. Because the effective PSF of STED microscopy exceeds the diffraction limit, dense stripes with high spatial frequencies exceeding the observable passband of microscopes were generated on the sample. To reconstruct an isotropic STED-psSIM image, nine STED-based scanning illumination patterns with three orientations were required. If aiming for the same level of resolution, STED-psSIM offers the advantage of reduced laser power loss, making it well-suited for superresolution imaging studies in live cells. The method was applied for imaging fluorescent beads and labeled cellular actin, and the resolutions obtained using confocal, STED, and STED-psSIM techniques were compared.

2. Results

2.1. Experimental setup

The principle of STED-psSIM is shown in Supplementary Notes 1 and 2 (see Supplementary Material). The schematic diagram of STED-psSIM is shown in Fig. 1(a). A 635 nm CW laser (LDH-D-C-635M, Picoquant) was used for the excitation beam, and a near-infrared femtosecond pulsed laser (UltraII, Chameleon) running at a repetition rate of 80 MHz was used for the depletion beam. The excitation beam passed through a half-wave plate (HWP) and an electro-optic modulator (EOM, Model 350, Conoptics) to produce a sinusoidal intensity-modulated beam with a modulation depth of more than 0.34. The depletion laser beam passed through a vortex phase plate (VPP-1C, LBTEK) to generate a doughnut-shaped spot and was subsequently overlaid with the excitation beam using two dichroic mirrors (DM2, ET760lpxr-UF2 and DM1, ZT647rdc-UF2, Chroma). A quarter-wave plate (WPQ10M-780, Thorlabs) was used to generate a circularly polarized STED beam. Using right-handed circular polarization for depletion and detection yielded a uniform effective resolution increase in the lateral directions of the focal plane of the objective lens. The relationship among the excitation beam, the depletion beam, and the fluorescence signal in

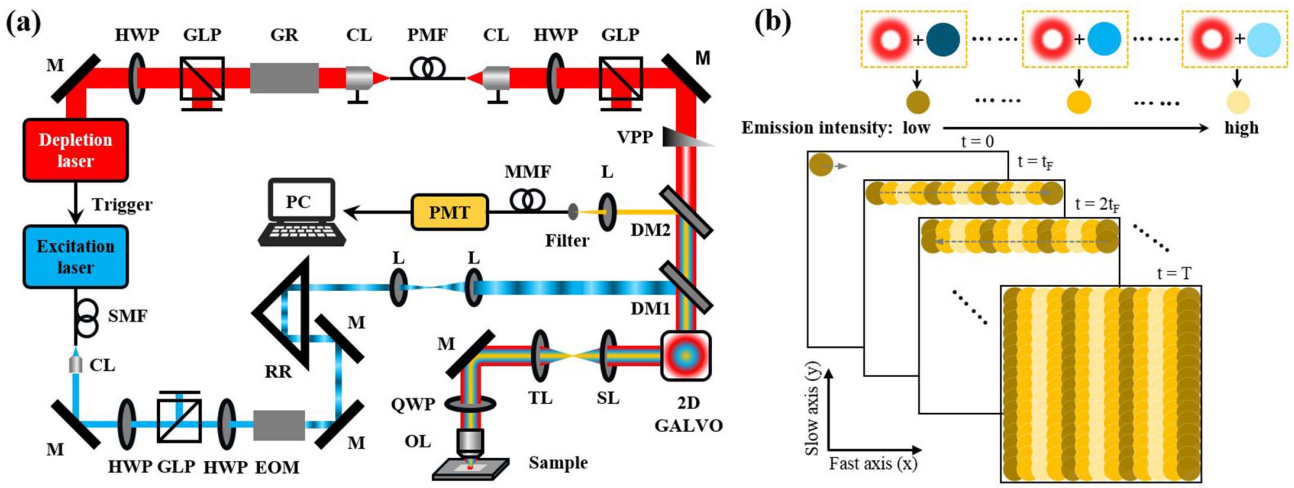

Fig. 1. (a) Schematic diagram of STED-psSIM; (b) relationship among the excitation beam, the depletion beam, and the fluorescence signal in the temporal and spatial domain.

temporal and spatial domain is shown in Fig. 1(b). The combined beam was scanned by a 2D galvo scanner (Model 6210H, Cambridge Tech) driven by a DAQ card (PCI6110, NI) with sawtooth waves. The scanned beam then passed through a scanning lens (AC508-100-B, Thorlabs) and a tube lens (TTL200MP, Thorlabs) and was focused onto the imaging plane of the sample by a high numerical aperture (NA) objective (100×, NA 1.4, HCX PL Apo, Leica). To achieve strong fluorescence inhibition, the STED wavelength was set to 750 nm, and the fluorescence signal was collected by the same objective lens. After passing through the tube lens, scanning lens, and the 2D galvo scanner, the fluorescence signal was detected confocally using a multimode fiber. A bandpass filter (ET690/50 m, Chroma) as emission filter was used to reject stray and ambient light before PMT (H7422-50, Hamamatsu). Excitation illumination patterns were generated by combining the scanning of the excitation beam and the sinusoidal modulation of its intensity[25]. The phase and orientation of the illumination pattern can be changed by varying the phase and period of sine waves that are used to drive the EOM. To obtain high-resolution isotropic images, three orientation patterns are sufficient for the reconstruction[26]. The scanning illumination patterns with orientations of 15°, 75°, and 135° with respect to the fast axis of the scanners are used here. For each orientation, three patterns were produced with different initial phases, i.e., 0, $2\pi/3$, and $4\pi/3$.

In our experiments, we wrote custom software using MATLAB. Based on the traditional SIM reconstruction algorithm[27], nine raw structured fluorescence illumination images were utilized to reconstruct an isotropic STED-psSIM image. The process includes the following four major steps. (i) Rescaling raw images. To compensate for intensity fluctuations of light source and photobleaching, we rescaled the raw images to equalize their total background-subtracted intensity. (ii) Calculating the separated frequency components based on three raw images of each direction. We slightly trimmed the spectra using the apodization method to reduce the noise and edge artifacts introduced by discrete Fourier transform. (iii) Shifting the separated frequency components in the three directions back to their initial positions, and then linearly integrating them according to their weight. (iv) Wiener-filtering the added spectrum and reconstructing a superresolution image.

2.2. Experimental results

To analyze the resolution improvement capability, STED-psSIM, confocal microscopy, and conventional STED microscopy were used to image 23 nm-sized beads (Bead R, GATTA) whose sizes were below the theoretically possible resolution of STED-psSIM. A 635 nm excitation light with 5.6 μW power and a 750 nm STED light with 30 mW power were used for STED and STED-psSIM. The images were reconstructed for different imaging methods, and the normalized intensity curves along the blue and yellow dashed lines passing through the center of a diffracted image point are shown in Fig. 2. As shown in Fig. 2(e), the two adjacent fluorescent beads (120 nm apart) were clearly distinguished by STED-psSIM. The average FWHMs of the beads for a confocal microscope, STED, and STED-psSIM were 193, 117, and 74 nm, respectively, as shown in Fig. 2(f). Compared with conventional STED microscopy, STED-psSIM showed a 1.58-fold improvement in lateral resolution.

To investigate the potential of STED-psSIM for biological imaging, an Abberior STAR READ-stained NPC was imaged using the three aforementioned imaging modes. Results are shown in Fig. 3(a); locally enlarged images are shown in Fig. 3(c). Abberior STAR READ is a traditional fluorophore used for STED imaging. A wavelength between 630 and 650 nm is recommended for excitation light, and a depletion wavelength of around 750 to 800 nm is recommended for STED light. In the experiments, the 635 nm excitation light with 5.6 μW power was used for all images, and the 750 nm STED light with 15 mW power were used for STED and STED-SIM. Figure 3(c) shows that

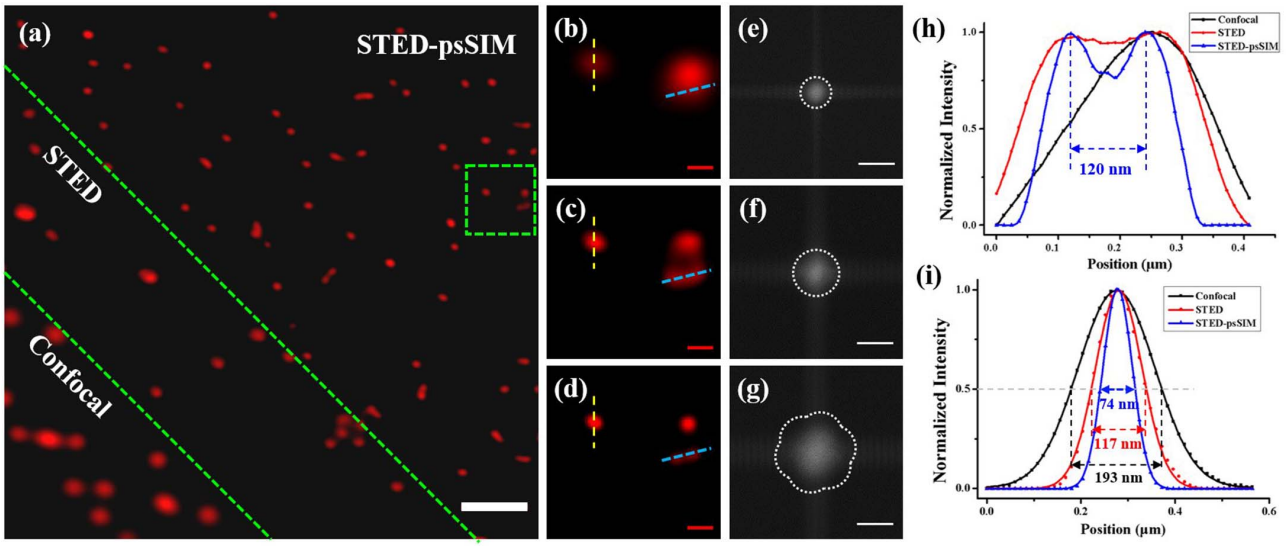

Fig. 2. Comparison of imaging resolutions of confocal microscopy, STED microscopy, and STED-psSIM. (a) Images of 23 nm fluorescent beads captured by the confocal microscopy (lower left), STED microscopy (middle), and STED-psSIM (upper right) separated by a dashed green line; (b)–(d) magnified view of the area encircled by the green dashed box in (a): (b) confocal microscopy, (c) STED microscopy, and (d) STED-psSIM[28]; (e)–(g) observable spatial frequency regions obtained by Fourier transforming images in (b)–(d); (h), (i) normalized intensity profiles of fluorescence beads along the (h) blue and (i) yellow dashed lines in (b)–(d), respectively. The profiles show average FWHMs of 193, 117, and 74 nm. Scale bars, 1 μm in (a) and 0.2 μm in (b)–(d).

STED-SIM can clearly distinguish the two very close samples [108 nm apart, Fig. 3(d)], but both the confocal microscope and STED are unable to do so. Therefore, STED-SIM can improve spatial resolution and enhance the visibility of the structure of NPC.

Similarly, to test STED-psSIM's capabilities in the field of cell imaging, we imaged red-fluorescent Alexa Fluor 647-labeled actin in a commercial huFIB cell sample (GATTA-Cells 3c, GATTA) with the three imaging modes. The results are shown in Fig. 3(b); a locally enlarged image is shown in Fig. 3(e). In the experiments, a 635 nm excitation light with 5.6 μW power and a 750 nm STED light with 15 mW power were used for STED microscopy and STED-psSIM. The STED-psSIM can clearly distinguish the two closely placed actins [84 nm apart, shown in Fig. 3(f)], but both the confocal microscopy and STED microscopy were unable to do so. Therefore, STED-psSIM has improved the spatial resolution and enhanced the visibility of the structures of actin. Figure 3(g) shows the signal-to-background ratio (SBR) of the two biological samples in the three methods. The STED-psSIM image has the highest signal-to-noise ratio (SNR), which further verifies that STED-psSIM has the highest resolution compared with confocal and STED microscopy.

3. Conclusion

To reduce the effect of the sine pattern rotation, we changed only the driving function of EOM without rotating samples; other information, including the control parameters of the 2D galvo scanner and acquisition parameters of PMT were unchanged in experiments. Therefore, all nine frames of raw structured fluorescence illumination image data for STED-psSIM were continuously obtained after the homemade control program was executed once, without rotating samples. All control signals were generated by a PCI6110 card: a 6.55 kHz sine wave was used to drive the EOM to generate a 15°-oriented structured illumination pattern, 23.8 kHz for a 75°-oriented structured illumination pattern, and 17.5 kHz for a 135°-oriented structured illumination pattern. 1024-Hz and 2 Hz sawtooth waves were used to synchronously drive the 2D galvo scanner. Thus, a sinusoidally scanning structured illumination pattern with a spatial period of 132 nm was generated, which corresponds to a theoretical resolution improvement of 1.88-fold. The acquisition time of each raw sinusoidally structured fluorescence illumination pattern was 0.5 s, and the field of view was 6 μm × 6 μm.

To summarize, we have developed a STED-psSIM that improved the resolution without increasing the excitation light power. Although STED microscopes have indeed showcased extraordinary capabilities in achieving resolutions on the order of tens of nanometers, it is crucial to note that the improvement of resolution in STED microscopy is indeed associated with the erasure light, and specifically, the higher the erasure light power, the greater the potential for improved resolution. This is a fundamental principle of STED microscopy, where the focused erasure beam selectively de-excites the fluorophores in the periphery of the excitation spot, thereby reducing the effective PSF and enhancing resolution. However, as mentioned earlier, the use of higher erasure light power can pose challenges related to photodamage and other sample-related considerations. Balancing these factors is a key consideration in optimizing STED microscopy experiments for specific applications. Our proposed method involves using STED-psSIM under the same optical power to achieve higher resolution, all while effectively

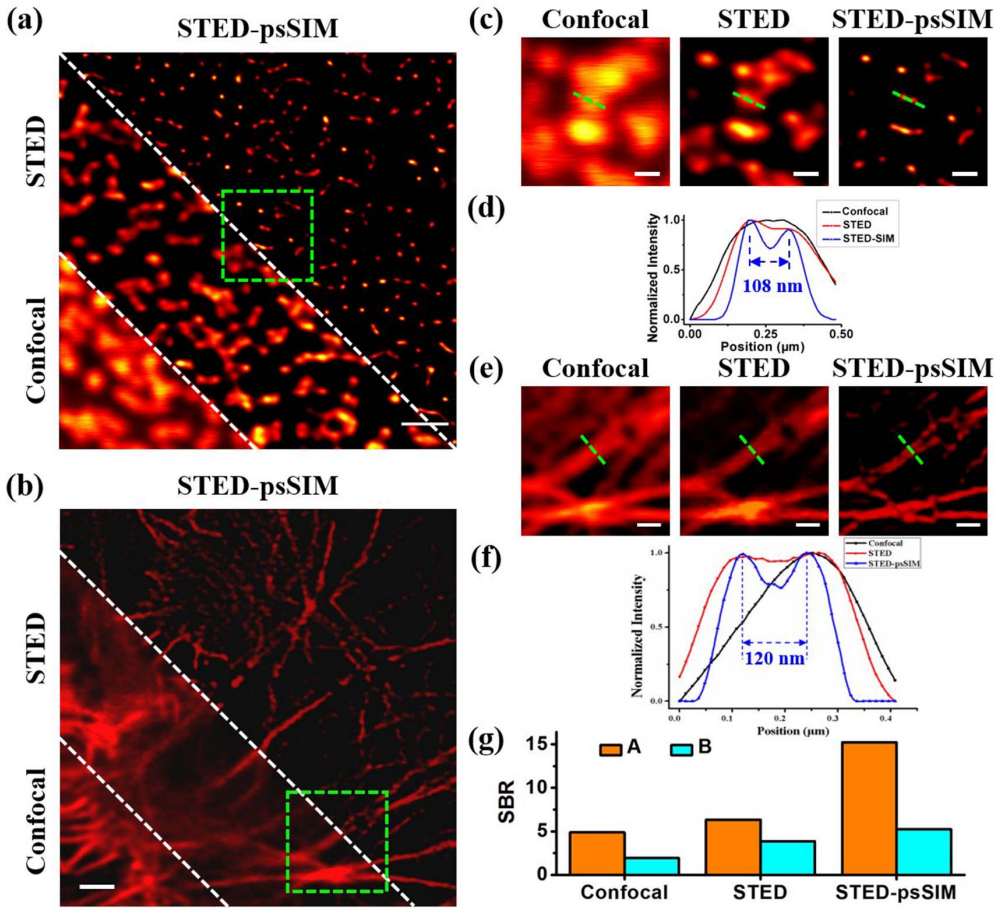

Fig. 3. Resolution improvement in STED-psSIM for biological imaging. (a) Images of NPC and (b) labeled actin in huFIB cells captured by confocal microscope (lower left), STED (middle), and STED-SIM (upper right) separated by two dashed green lines; (c) and (e) magnified view of the area encircled by the dashed box in (a) and (b); (d) and (f) normalized intensity profiles along the green dashed lines in (c) and (e), respectively; (g) SBR of the two biological samples in the three methods. Scale bars, 1 μm in (a), (b), 0.4 μm in (c), and 0.2 μm in (e).

reducing the intensity of the erasure light. This strategic approach enhances the suitability of STED for live-cell imaging, addressing the crucial balance between resolution enhancement and minimizing the impact of the erasure light on living samples.

Theoretically, the resolution of STED-psSIM is twice higher than that of STED microscopy. In our experiments, a lateral resolution of 74 nm was achieved, which is a 1.58-fold improvement over conventional STED. There are three main aspects that reduce the experimental resolution. First, the STED light path may have a minor system aberration or residual beam misalignment. Second, the illumination fringe parameters (i.e., initial phase, fringe period, phase difference) used in the image reconstruction process are estimated based on the original images, thus introducing estimation errors. Additionally, photobleaching will reduce quality and resolution in the reconstructed images. If the parameters of point-scanning structured illumination patterns in our experiments and reconstruction process were optimized, the resolution can be further improved.

As far as we understand, if both the excitation beam and STED beam are modulated, similar to Ref. [18], the SNR of each excitation spot will change with the STED modulation function, resulting in different resolutions of each sample spot, which will affect the image quality of STED-psSIM. Therefore, we prefer to use a constant energy density of the STED beam. Although improving the resolution in our STED-psSIM comes at the expense of increasing the number of STED imaging frames, resonant scanners or multifocal excitation schemes could be used to improve the imaging speed in the future[29]. We noted that the requirement of more frames (nine times) than normal STED methods may cause photobleaching. We will address this issue by developing photobleaching-resistant dyes in future studies. The method of resolution improvement could be attributed to the development of the superresolution technologies. This STED-psSIM provides an efficient high-resolution imaging strategy for visualizing cellular fine structures.

Acknowledgements

This work was supported by the National Natural Science Foundation of China (Nos. 62275168, 62275164, 61775148,

and 61905145), the National Key Research and Development Program of China (No. 2022YFA1206300), the Guangdong Natural Science Foundation and Province Project (Nos. 2021A1515011916 and 2023A1515012250), the Foundation from Department of Science and Technology of Guangdong Province (No. 2021QN02Y124), the Foundation from Department of Education of Guangdong Province (No. 2023ZDZX2052), the Shenzhen Science and Technology R&D and Innovation Foundation (No. JCYJ20200109105608771), the Shenzhen Key Laboratory of Photonics and Biophotonics (No. ZDSYS20210623092006020), and the Medical-Engineering Interdisciplinary Research Foundation of Shenzhen University.

References

1. M. J. Rust, M. Bates, and X. W. Zhuang, "Sub-diffraction-limit imaging by stochastic optical reconstruction microscopy (STORM)," Nat. Methods **3**, 793 (2006).
2. E. Betzig, G. H. Patterson, R. Sougrat, *et al.*, "Imaging intracellular fluorescent proteins at nanometer resolution," Science **313**, 1642 (2006).
3. S. T. Hess, T. P. K. Girirajan, and M. D. Mason, "Ultra-high resolution imaging by fluorescence photoactivation localization microscopy," Biophys. J. **91**, 4258 (2006).
4. W. E. Moerner and M. Orrit, "Illuminating single molecules in condensed matter," Science **283**, 1670 (1999).
5. B. Huang, H. Babcock, and X. Zhuang, "Breaking the diffraction barrier: super-resolution imaging of cells," Cell **143**, 1047 (2010).
6. G. T. Dempsey, J. C. Vaughan, K. H. Chen, *et al.*, "Evaluation of fluorophores for optimal performance in localization-based super-resolution imaging," Nat. Methods **8**, 1027 (2011).
7. M. G. L. Gustafsson, "Surpassing the lateral resolution limit by a factor of two using structured illumination microscopy," J. Microsc. **198**, 82 (2000).
8. R. Heintzmann and M. G. L. Gustafsson, "Subdiffraction resolution in continuous samples," Nat. Photonics **3**, 362 (2009).
9. Z. J. Wang, T. Y. Zhao, Y. A. Cai, *et al.*, "Rapid, artifact-reduced, image reconstruction for super-resolution structured illumination microscopy," Innovation **4**, 100425 (2023).
10. Z. J. Wang, T. Y. Zhao, H. W. Hao, *et al.*, "High-speed image reconstruction for optically sectioned, super-resolution structured illumination microscopy," Adv. Photonics **4**, 026003 (2022).
11. J. Lu, W. Min, J. A. Conchello, *et al.*, "Super-resolution laser scanning microscopy through spatiotemporal modulation," Nano Lett. **9**, 3883 (2009).
12. B. E. Urban, J. Yi, S. Y. Chen, *et al.*, "Super-resolution two-photon microscopy via scanning patterned illumination," Phys. Rev. E **91**, 33 (2015).
13. X. M. Zheng, L. Wang, M. T. Wang, *et al.*, "Resolution improvement of structured illumination microscopy using non-diffraction-limited point-scanned fluorescence fringe," Laser Photonics Rev. **17**, 2200796 (2023).
14. L. Wang, J. Zhou, M. T. Wang, *et al.*, "Improvement in resolution of multiphoton scanning structured illumination microscopy via harmonics," Engineering **12**, 65 (2021).
15. M. T. Wang, L. Wang, X. M. Zheng, *et al.*, "Nonlinear scanning structured illumination microscopy based on nonsinusoidal modulation," J. Innov. Opt. Health Sci. **14**, 2142002 (2021).
16. S. W. Hell and J. Wichmann, "Breaking the diffraction resolution limit by stimulated-emission-depletion fluorescence microscopy," Opt. Lett. **19**, 780 (1994).
17. T. A. Klar and S. W. Hell, "Subdiffraction resolution in far-field fluorescence microscopy," Opt. Lett. **24**, 954 (1999).
18. X. S. Yang, Z. G. Yang, Z. Y. Wu, *et al.*, "Mitochondrial dynamics quantitatively revealed by STED nanoscopy with an enhanced squaraine variant probe," Nat. Commun. **11**, 3699 (2020).
19. H. Zhang, M. Zhao, and L. L. Peng, "Nonlinear structured illumination microscopy by surface plasmon enhanced stimulated emission depletion," Opt. Express **19**, 24783 (2011).
20. F. Dake, S. Nakayama, and Y. Taki, "Theoretical assessment of two-dimensional nonlinear structured illumination microscopy based on structured excitation and structured stimulated emission depletion," Opt. Rev. **22**, 598 (2015).
21. S. Puthukodan, E. Murtezi, J. Jacak, *et al.*, "Localization STED (LocSTED) microscopy with 15 nm resolution," Nanophotonics **9**, 783 (2020).
22. M. F. Gao, R. Maraspini, O. Beutel, *et al.*, "Expansion stimulated emission depletion microscopy (ExSTED)," ACS Nano **12**, 4178 (2018).
23. R. Q. Li, X. Z. Chen, Z. X. Lin, *et al.*, "Expansion enhanced nanoscopy," Nanoscale **10**, 17552 (2018).
24. D. Kim, T. Kim, J. Lee, *et al.*, "Amplified expansion stimulated emission depletion microscopy," ChemBioChem **20**, 1260 (2019).
25. C. H. Yeh and S. Y. Chen, "Resolution enhancement of two-photon microscopy via intensity-modulated laser scanning structured illumination," Appl. Opt. **54**, 2309 (2015).
26. X. M. Zheng, J. Zhou, L. Wang, *et al.*, "Current challenges and solutions of super-resolution structured illumination microscopy," APL Photonics **6**, 020901 (2021).
27. X. Zhou, M. Lei, D. Dan, *et al.*, "Image recombination transform algorithm for superresolution structured illumination microscopy," J. Biomed. Opt. **21**, 96009 (2016).
28. J. S. Di Martino, A. R. Nobre, C. Mondal, *et al.*, "A tumor-derived type III collagen-rich ECM niche regulates tumor cell dormancy," Nat. Cancer **3**, 90 (2022).
29. Y. Xue and P. T. C. So, "Three-dimensional super-resolution high-throughput imaging by structured illumination STED microscopy," Opt. Express **26**, 20920 (2018).